

ПИ
B60/рб

行 36巻4号平成25年4月1日発行 昭和55年4月26日 第3種郵便物認可 ISSN 0918-6158

Biological and Pharmaceutical Bulletin

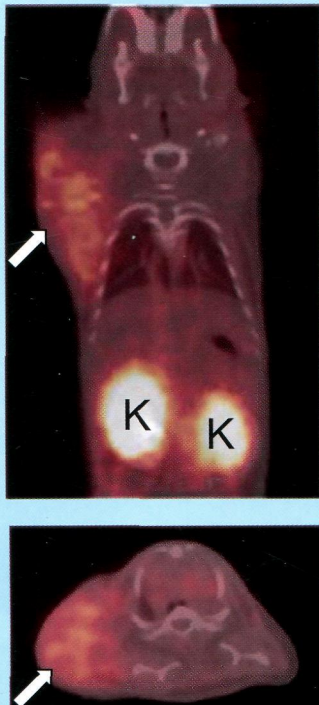
April 2013

BPBLEO 36 (4) 501–690 (2013)

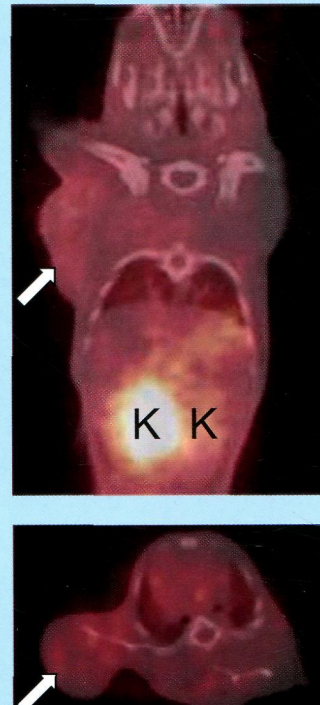
Vol. 36 No. 4

Biological and Pharmaceutical Bulletin succeeds to Journal of Health Science from 2012.

^{68}Ga -DOTA-MN2



^{68}Ga -DOTA



Cover Figure $^{67/68}\text{Ga}$ -DOTA-MN2 for Hypoxic Tumor Imaging

pp. 602–608

Highlighted Paper • New Efficacies of EA in PQ-Induced Cytotoxicity
(Yong-Sik Kim *et al.*) pp. 609–615



THE PHARMACEUTICAL SOCIETY OF JAPAN

<http://bpb.pharm.or.jp>

Biological and Pharmaceutical Bulletin

Vol. 36, No. 4 April 2013

© Copyright, 2013, by the Pharmaceutical Society of Japan.

Contents

Review

A Model of the Central Regulatory System for Cough Reflex

A. Haji, S. Kimura, and Y. Ohi 501

Regular Articles

Cetylpyridinium Chloride Inhibits Receptor Activator of Nuclear Factor- κ B Ligand-Induced Osteoclast Formation

T. Zheng, L. Chen, A L. S. M. Noh, and M. Yim 509

Effects of Astragaloside IV on Action Potentials and Ionic Currents in Guinea-Pig Ventricular Myocytes

M.-M. Zhao, J.-S. Zhao, G.-L. He, X.-F. Sun, X.-S. Huang, and L.-Y. Hao 515

Activation of AMP-Activated Protein Kinase by a Plant-Derived Dihydroisosteviol in Human Intestinal Epithelial Cell

C. Muanprasat, L. Sirianant, S. Sawasvirojwong, S. Homvisasevongsa, A. Suksamrarn, and V. Chatsudthipong 522

Changes in Small Heat Shock Proteins HSPB1, HSPB5 and HSPB8 in Mitochondria of the Failing Heart Following Myocardial Infarction in Rats

T. Marunouchi, Y. Abe, M. Murata, S. Inomata, A. Sanbe, N. Takagi, and K. Tanonaka 529

Nobiletin Induces Inhibition of Ras Activity and Mitogen-Activated Protein Kinase Kinase/Extracellular Signal-Regulated Kinase Signaling to Suppress Cell Proliferation in C6 Rat Glioma Cells

K. Aoki, A. Yokosuka, Y. Mimaki, K. Fukunaga, and T. Yamakuni 540

Vascular Endothelial Growth Factor Modulates Voltage-Gated Na^+ Channel Properties and Depresses Action Potential Firing in Cultured Rat Hippocampal Neurons

G. Sun and Y. Ma 548

Effects of Cyanamide, an Aldehyde Dehydrogenase Type 2 Inhibitor, on Glyceryl Trinitrate- and Isosorbide Dinitrate-Induced Vasodilation in Rabbit Excised Aorta and in Anesthetized Whole Animal

T. Ishibashi, M. Nomura-Nakamoto, F. Abe, T. Masuoka, N. Imaizumi, J. Yoshida, T. Kawada, and M. Nishio 556

The Effect of Sex Hormones on Peroxisome Proliferator-Activated Receptor Gamma Expression and Activity in Mature Adipocytes

H. Sato, H. Sugai, H. Kurosaki, M. Ishikawa, A. Funaki, Y. Kimura, and K. Ueno 564

Decrease in Venous Irritation by Adjusting the Concentration of Injected Bendamustine

H. Watanabe, H. Ikesue, T. Tsujikawa, K. Nagata, M. Uchida, K. Suetsugu, N. Egashira, T. Muta, K. Kato, K. Takenaka, S. Ohga, T. Matsushima, M. Shiratsuchi, T. Miyamoto, T. Teshima, K. Akashi, and R. Oishi 574

Carvacrol Protects against Acute Myocardial Infarction of Rats via Anti-oxidative and Anti-apoptotic Pathways

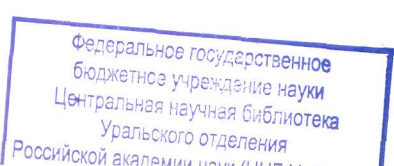
W. Yu, Q. Liu, and S. Zhu 579

Protective Effects of Apomorphine against Zinc-Induced Neurotoxicity in Cultured Cortical Neurons

H. Hara, A. Maeda, T. Kamiya, and T. Adachi 585

Corticosterone Suppresses the Proliferation of RAW264.7 Macrophage Cells via Glucocorticoid, But Not Mineralocorticoid, Receptor

Y. Nakatani, T. Amano, and H. Takeda 592



<i>In Vivo</i> Evaluation of a Radiogallium-Labeled Bifunctional Radiopharmaceutical, Ga-DOTA-MN2, for Hypoxic Tumor Imaging K. Sano, M. Okada, H. Hisada, K. Shimokawa, H. Saji, M. Maeda, and T. Mukai	602
* Antioxidant Action of Ellagic Acid Ameliorates Paraquat-Induced A549 Cytotoxicity Y.-S. Kim, T. Zerin, and H.-Y. Song	609
Hepatic Steatosis with Relation to Increased Expression of Peroxisome Proliferator-Activated Receptor- γ in Insulin Resistant Mice H. Satoh, N. Ide, Y. Kagawa, and T. Maeda	616
Different Diets Cause Alterations in the Enteric Environment and Trigger Changes in the Expression of Hepatic Cytochrome P450 3A, a Drug-Metabolizing Enzyme M. Tajima, N. Ikarashi, S. Igeta, T. Toda, M. Ishii, Y. Tanaka, Y. Machida, W. Ochiai, H. Yamada, and K. Sugiyama	624
Enzymatic Cleavage of the C-Glucosidic Bond of Puerarin by Three Proteins, Mn ²⁺ , and Oxidized Form of Nicotinamide Adenine Dinucleotide K. Nakamura, K. Komatsu, M. Hattori, and M. Iwashima	635
Reversal Effect of Arsenic Sensitivity in Human Leukemia Cell Line K562 and K562/ADM Using Realgar Transforming Solution X. Wang, X. Zhang, Z. Xu, Z. Wang, X. Yue, and H. Li	641
Consumption of a High-Fat Diet during Pregnancy Changes the Expression of Cytochrome P450 in the Livers of Infant Male Mice M. Tajima, N. Ikarashi, T. Okaniwa, Y. Imahori, K. Saruta, T. Toda, M. Ishii, Y. Tanaka, Y. Machida, W. Ochiai, H. Yamada, and K. Sugiyama	649
High-Throughput and Sensitive Assay for Amphotericin B Interaction with Lipid Membrane on the Model Membrane Systems by Surface Plasmon Resonance M. Onishi and H. Kamimori	658
Peptide Structure Modifications: Effect of Radical Species Generated by Controlled Gamma Ray Irradiation Approach R. de F. F. Vieira, D. T. Nardi, N. Nascimento, J. C. Rosa, and C. R. Nakae	664
Interindividual Variations in Aprepitant Plasma Pharmacokinetics in Cancer Patients Receiving Cisplatin-Based Chemotherapy for the First Time S. Motohashi, Y. Mino, K. Hori, T. Naito, S. Hosokawa, H. Furuse, S. Ozono, H. Mineta, and J. Kawakami	676

Notes

Plasma and Serum from Nonfasting Men and Women Differ in Their Lipidomic Profiles M. Ishikawa, Y. Tajima, M. Murayama, Y. Senoo, K. Mackawa, and Y. Saito	682
Effects of Moxifloxacin on Serum Glucose Concentrations in Rats Y. Ishiwata, Y. Takahashi, M. Nagata, and M. Yasuhara	686

About the cover: Based on the concept of bifunctional radiopharmaceuticals, a radiogallium-labeled metronidazole derivative, Ga-DOTA-MN2, was developed as a candidate SPECT (⁶⁷Ga) and generator-produced PET (⁶⁸Ga) radiopharmaceutical for hypoxia imaging. We performed small-animal PET studies with ⁶⁸Ga-DOTA-MN2 in mice bearing mouse mammary carcinoma (FM3A). Figure shows merged images of PET and CT at 1 h after injection of ⁶⁸Ga-DOTA-MN2 or ⁶⁸Ga-DOTA. The hypoxic tumor in the right flank was clearly visualized 1 h after injection of ⁶⁸Ga-DOTA-MN2 with high contrast to normal tissues, except the kidneys, while ⁶⁸Ga-DOTA showed low accumulation in the tumor. Arrows and K indicate tumors and kidneys, respectively. See the article by Sano *et al.* on page 602 of this issue.

* *Highlighted Paper selected by Editor-in-Chief*

The selection is based upon originality, scientific contributions, methodological pertinence, and composition.